

**Collision-induced activation of the  $\beta$ -hydride elimination reaction of isobutyl iodide dissociatively chemisorbed on Al(111)**

Shrikant P. Lohokare, Elizabeth L. Crane, Lawrence H. Dubois, and Ralph G. Nuzzo

Citation: *The Journal of Chemical Physics* **108**, 8640 (1998); doi: 10.1063/1.476294

View online: <http://dx.doi.org/10.1063/1.476294>

View Table of Contents: <http://scitation.aip.org/content/aip/journal/jcp/108/20?ver=pdfcov>

Published by the [AIP Publishing](#)

---

**Articles you may be interested in**

[Hot precursor reactions during the collisions of gas-phase oxygen atoms with deuterium chemisorbed on Pt\(100\)](#)  
J. Chem. Phys. **126**, 134704 (2007); 10.1063/1.2713111

[Quantum study of Eley-Rideal reaction and collision induced desorption of hydrogen atoms on a graphite surface. I. H-chemisorbed case](#)  
J. Chem. Phys. **124**, 124702 (2006); 10.1063/1.2177654

[Surface induced dissociations of protonated ethanol monomer, dimer and trimer ions: Trimer break-down graph from the collision energy dependence of projectile fragmentation](#)  
J. Chem. Phys. **118**, 7090 (2003); 10.1063/1.1556851

[The chemisorption and dissociation of ethylene on Pt{111} from first principles](#)  
J. Chem. Phys. **110**, 4699 (1999); 10.1063/1.478356

[Collision induced desorption and dissociation of O<sub>2</sub> chemisorbed on Ag\(001\)](#)  
J. Chem. Phys. **109**, 2490 (1998); 10.1063/1.476820

---



# Collision-induced activation of the $\beta$ -hydride elimination reaction of isobutyl iodide dissociatively chemisorbed on Al(111)

Shrikant P. Lohokare and Elizabeth L. Crane

*School of Chemical Sciences, Department of Materials Science and Engineering and the Frederick Seitz Materials Research Laboratory, University of Illinois at Urbana-Champaign, Urbana, Illinois 61801*

Lawrence H. Dubois

*Defense Advanced Research Projects Agency, Arlington Virginia 22203, and MIT Lincoln Laboratories, Lexington, Massachusetts 02173*

Ralph G. Nuzzo

*School of Chemical Sciences, Department of Materials Science and Engineering and the Frederick Seitz Materials Research Laboratory, University of Illinois at Urbana-Champaign, Urbana, Illinois 61801*

(Received 25 September 1997; accepted 19 February 1998)

The collision-induced activation of the endothermic surface reaction of isobutyl iodide chemisorbed on an Al(111) surface is demonstrated using inert-gas, hyperthermal atomic beams. The collision-induced reaction (CIR) is highly selective towards promoting the  $\beta$ -hydride elimination pathway of the chemisorbed isobutyl fragments. The cross section for the collision-induced reaction was measured over a wide range of energies (14–92 kcal/mol) at normal incidence for Ar, Kr, and Xe atom beams. The CIR cross section exhibits scaling as a function of the normal kinetic energy of the incident atoms. The threshold energy for the  $\beta$ -hydride elimination reaction calculated from the experimental results using a classical energy transfer model is  $\sim 1.1$  eV ( $\sim 25$  kcal/mol). This value is in excellent agreement with that obtained from an analysis of the thermally activated kinetics of the reaction. The measured cross section shows a complex dependence on both the incident energy of the colliding atom and the thermal energy provided by the surface where the two energy modes are interchangeable. The dynamics are explained on the basis of an impulsive, bimolecular collision event where the  $\beta$ -hydride elimination proceeds via a possible tunneling mechanism. The threshold energy calculated in this manner is an upper limit given that it is derived from an analysis which ignores excitations of the internal modes of the chemisorbed alkyl groups.

© 1998 American Institute of Physics. [S0021-9606(98)02420-9]

## INTRODUCTION

The effects of surface structure and temperature on the reactivity of adsorbates under equilibrium conditions have been studied extensively.<sup>1–3</sup> These studies have yielded a good understanding of thermally activated surface processes important in diverse areas of technology, especially as regards materials growth and catalysis.<sup>1–7</sup> The dynamical effects of energetic atom or molecule collisions with surfaces have received much less attention (in part due to the complex experimental techniques needed to study such phenomena), and as a result are less well understood. Molecular beams producing high velocity atoms or molecules in the hyperthermal energy range can be coupled with sensitive, ultrahigh vacuum spectroscopies in order to investigate the effect of collision-induced processes at the microscopic level.<sup>8</sup> Supersonic beams have two useful qualities: They can be generated with a narrow velocity distribution and a wide range of translational energies.<sup>9</sup> The utility of the beam as an experimental tool stems from the fact that the kinetic energy of the collision can be utilized to overcome the activation barrier of a surface reaction. The conditions achieved can approximate the high energy collisions which occur at high pressure, temperature, or in plasmas and allow activated and/or low probability processes to be simulated inside an ultrahigh vacuum

environment.<sup>8</sup> For example, kinetic-energy enhanced activation of neutral species finds important applications in the technologies used for the deposition<sup>10–12</sup> and etching of silicon.<sup>13</sup> Translational activation of molecular precursors is not a completely general strategy for materials growth, however, since in many cases thermal decomposition may result from the use of high nozzle temperatures in the beam source.

Complementing translational activation is the closely related process of collision-induced activation, in which energy transfer to the adsorbate is effected by an energetic collision involving a second gas-phase species of high translational energy. An early discussion of the dynamics of collision-induced activation of surface bound adsorbates was presented by Zeiri, Low, and Goddard.<sup>14</sup> These results, based on classical stochastic trajectory theory, have been expanded in more recent studies by Zeiri *et al.*,<sup>15,16</sup> and Rabitz *et al.*<sup>17,18</sup> From an experimental stand point, Ceyer *et al.* demonstrated both the collision-induced desorption (CIDE)<sup>19–23</sup> and collision induced dissociation (CID)<sup>21–25</sup> of methane on a Ni(111). They proposed a model for the kinetic energy transfer from the incident inert gas atom to the physisorbed CH<sub>4</sub> molecule involving an impulsive, bimolecular collision which induces the activated dissociative adsorption of the CH<sub>4</sub>. These investigations have inspired more recent

studies on other small, symmetric adsorbates, including ammonia<sup>26,27</sup> and ethylene<sup>28</sup> on Pt(111) and water on Ru(001).<sup>29</sup> Levis *et al.*, made a direct measurement of the threshold energy for collision-induced desorption of NH<sub>3</sub> from the Pt(111) surface by a beam of neutral, hyperthermal Ar atoms and found that the total energy scaling of the desorption cross section holds for various angles of incidence.<sup>26</sup> In contrast, Asscher *et al.*, observed efficient kinetic energy dissipation by the hydrogen bonded network of a dense monolayer of water on the Ru(001) surface in an investigation of H<sub>2</sub>O desorption effected by collisions with energetic Kr atoms.<sup>29</sup> Despite this considerable progress, the feasibility of effecting collision-induced surface reactions in large, multiatomic adsorbates (both physisorbed and chemisorbed) remains a largely unexplored area of research. One expects intuitively that the probability of bond dissociation by means of an energetic collision will be reduced given the increased possibilities for internal energy dissipation and the exceedingly rapid rates of both energy transfer and quenching. However, it must be pointed out that the cross sections for certain types of selective bond scission can be substantial. Levis and Velic,<sup>28</sup> for example, have demonstrated that the collision-induced desorption of ethylene from the Pt(111) surface is selective in desorbing the  $\pi$ -bonded form of C<sub>2</sub>H<sub>4</sub> over that of the  $\sigma$ -bonded species. The ability to activate reactions in complex adsorbates would be of great utility in exploring activated chemisorption phenomena such as those involved in the technologically important areas of catalysis<sup>3,8</sup> and materials growth and processing.<sup>4,5,8,30–32</sup> The present study explores the feasibility of using collision-induced processes to understand the dynamics and energetics of reactions involved in the chemical vapor deposition (CVD) of aluminum.

Aluminum metallization in very large scale integrated (VLSI) devices is of significant technological importance.<sup>5,33</sup> One of the fabrication processes of current commercial interest is the chemical vapor deposition and growth of aluminum thin films by the surface-mediated thermal decomposition of triisobutylaluminum (TIBA).<sup>5,6,33–35</sup> The dissociation and reaction of TIBA on a non-native substrate (e.g., Si or SiO<sub>2</sub>)<sup>33,36</sup> is activated and thus an understanding of the nucleation chemistry and nucleation morphology is not easy to study in UHV. This deficit is significant given that the growth-rate hysteresis and morphology are strongly determined by these early events and thus of central importance in determining the lifetimes (which are sensitive to microstructure) of devices so constructed.<sup>5,32</sup> A goal of the research reported here is to develop a better understanding of the mechanisms and energetics involved in the reaction-limited nucleation of Al–CVD (and other) thin films. In this report, we examine the feasibility of using hyperthermal, inert gas atom beams to activate large surface-bound organometallic fragments, such as those that might be found in Al–CVD processes involving TIBA.<sup>6</sup> The beam-induced reactions of a covalently bound isobutyl group are used as a model to explore this possibility. The present work is advantaged by the fact that useful models of isobutyl surface intermediates can be prepared easily by the dissociative chemisorption of isobutyl iodide on an aluminum surface.<sup>37</sup>

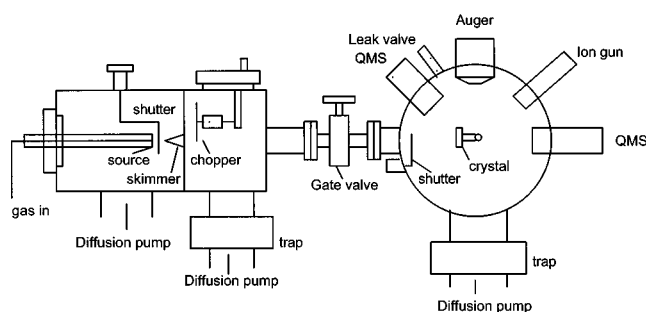


FIG. 1. A schematic sketch of the molecular beam source, differentially pumped stages and the scattering chamber.

The thermal chemistries of the surface bound isobutyl and iodine moieties were originally studied by Bent *et al.*<sup>37</sup> In the study described here, neutral, inert-gas (Xe, Kr, and Ar) beams with energies in the range of 0.5–4 eV were scattered off of a monolayer of isobutyl groups chemisorbed on Al(111). The experimental results suggest that the CID process predominantly promotes the  $\beta$ -hydride elimination reaction. The value of the activation barrier for the process is estimated to be  $\sim 1.1$  eV ( $\sim 25$  kcal/mol), in good agreement with the thermal barrier measured by temperature programmed reaction spectroscopy (TPRS).

## EXPERIMENTAL APPARATUS AND TECHNIQUES

The apparatus used in these investigations, illustrated in Fig. 1, combines a supersonic molecular beam with several UHV surface analytical tools. Specific details of the latter techniques have been described elsewhere.<sup>38</sup> The features pertinent to the CID studies are described below.

As shown in Fig. 1, the chamber has three main vacuum stages—two stages are employed in the beam generation and the third serves as the scattering and analytical chamber. The supersonic molecular beam source is housed in the first stage of the differentially pumped two stage beam chamber. The beam is formed by the continuous adiabatic expansion of the gas at high stagnation pressures from a 25  $\mu$  molybdenum aperture (Ladd Optics) mounted by furnace brazing in a stainless steel seat which in turn is welded to steel tubing conveying the gas. The aperture seat and the connected tubing is enclosed inside a cylindrical copper block with grooves holding tungsten wire insulated with ceramic. The wire was used to (resistively) heat the beam source from room temperature to  $\sim 850$  K to adjust the incident beam energy. The entire source assembly was mounted on a X–Y–Z translational manipulator. Temperatures were measured using a chromel–alumel thermocouple spot welded to the nozzle edge. The beam source chamber was pumped by a 10 in. diffusion pump. A 400  $\mu$  diameter nickel skimmer (model 1, Beam Dynamics) mounted on the inside wall of the first stage facing the source was used to form the beam. The skimmer–nozzle distance was  $\leq 1$  cm and was adjusted to optimize the beam intensity and velocity distribution by minimizing skimmer interference effects.<sup>39,40</sup> A collimator centered in a double sided flange separating the differentially pumped stages from the scattering chamber was used to fur-

ther collimate the expanding beam to a diameter of  $\sim 1.5$  cm at the sample. This ensures that the crystal is flooded with a uniform gas flow. A manual shutter attached to a rotary motion feed-through was used to shunt the beam flow through the skimmer in order to measure and minimize the background gas load. A similar shutter was also housed at the entry point inside the scattering chamber in order to measure the effusive load contributed by the beam source.

The scattering chamber is pumped by a 10 in. diffusion pump (5000 L/s) with a liquid nitrogen trap. Additional pumping is provided by a titanium sublimation pump and a 540 L/s turbomolecular pump. The base pressure of the UHV chamber is typically  $\leq 2 \times 10^{-10}$  Torr. The chamber is equipped with two quadrupole mass spectrometers (VG SXP 300 Quadrupoles), one in line with the beam axis and the other at  $45^\circ$  with reference to the beam axis, a cylindrical mirror analyzer (CMA) with a coaxial electron gun (Physical Electronics) for Auger electron spectroscopy (AES), an ion gun (Physical Electronics) for sputtering the crystal, a Bayard-Alpert type ionization gauge (Varian), and a precision leak valve (Duniway). Both mass spectrometers are shrouded and differentially pumped by 30 L/s ion pumps (Varian) and liquid nitrogen cold shields. The coaxial mass spectrometer was used for the time of flight (TOF) velocity distribution analysis of the supersonic molecular beam and for temperature programmed reaction spectroscopy. Specific details regarding sample preparation and TPRS acquisition are provided elsewhere.<sup>41</sup>

The kinetic energy distribution of the beam was determined by a standard time of flight method.<sup>39</sup> The time of flight was measured between a rotating chopper in the second stage, at a distance of  $\sim 15$  cm from the nozzle, and the line-of-sight mass spectrometer in the scattering chamber. The distance between the chopper and the mass spectrometer is  $\sim 98$  cm. The chopper is an aluminum disk with two diagonally opposite, precision machined slits (1 cm long, 1 mm wide) mounted on a two way 800 Hz ac synchronous motor (Globe) which is controlled by a power supply with a variable frequency control. The chopper modulates the beam at 175 Hz with a gating function of  $5.85 \mu\text{s}$  FWHM. The output pulses of the mass spectrometer signal were collected in a pulse-counting mode using a multichannel scalar (EG&G Ortec MCS PCB) with 256 channels and temporal resolution of  $1 \mu\text{s}$ . The time base of the scalar is triggered by the signal from a light emitting diode/photodetector which determines the rotational position of the chopper slit and hence the span of the beam pulse in real time. The signal is averaged over typically 10 000 chopper counts to obtain the time of flight spectrum. The kinetic energy spread ( $\Delta E/E$  at FWHM) was typically  $\sim 40\%$ . To estimate the absolute beam flux, the mass spectrometer was calibrated for its relative sensitivity to Ar, Kr, and Xe. The flux weighted distribution was calculated using the Jacobian for conversion from time to velocity space.<sup>39,42</sup> The signals for the most common isotopes for Ar (40), Kr (84), and Xe (131) were calibrated against a fixed background pressure.<sup>43</sup> The absolute flux was calculated to be of the order of  $\sim (2 \pm 1) \times 10^{13}$  atoms/cm<sup>2</sup>/s. All gas mixtures (1% in 99.99995% pure He) were obtained from Matheson and were of certified

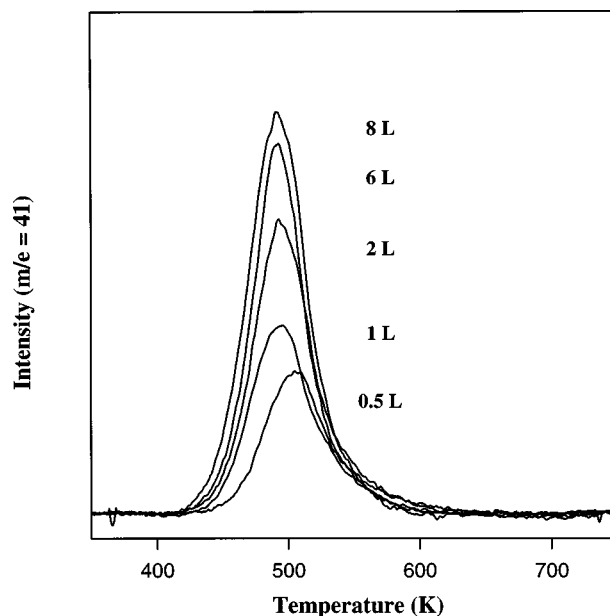


FIG. 2. TPR spectra of  $m/e=41$  as a function of exposures of isobutyl iodide to an Al(111) surface at 300 K.

concentrations. They were further tested for purity by mass spectroscopy and also by monitoring the exposed crystal with Auger electron spectroscopy for adsorbed contaminants deposited by the beam. Both these control tests showed the presence of little or no contaminants (such as  $\text{H}_2\text{O}$ ,  $\text{CO}_2$ , and  $\text{O}_2$ ).

## RESULTS

A study of the thermally activated reactions of isobutyl iodide on aluminum has been described.<sup>37</sup> The thermal dissociation of isobutyl iodide occurs efficiently on aluminum surfaces.<sup>37</sup> Physisorbed isobutyl iodide desorbs at  $\sim 180$  K but the chemisorbed alkyl and iodine fragments are stable on the surface to much higher temperatures ( $>450$  K). The thermal decomposition of the bound isobutyl group is facile at temperatures above 450 K. The reaction-limited evolution of the  $\beta$ -hydride elimination reaction product, isobutene, provides a convenient measure of the reaction kinetics. The depletion of the surface-bound isobutyl groups also results (to a lesser degree) from complex, associative metal etching reactions which yield both hydrido- and haloaluminum and isobutylaluminum complexes [AlI, diisobutylaluminum hydride (DIBAH), disobutylaluminum iodide (DIBAI)].<sup>41</sup> A common fragment useful for the mass spectroscopic detection of these desorption products (excluding AlI) is the ion  $\text{C}_3\text{H}_5^+$  ( $m/e=41$ ). The desorption yield detected at this mass can be used to estimate the cross sections of the collision-induced reactions described in this report. Figure 2 shows the TPRS data for  $m/e=41$  as a function of the increasing isobutyl iodide exposure to the Al(111) surface at 300 K. This data is included for the convenience of the reader. We note for later reference that the peak temperature shifts towards lower values with increasing coverages. The TPRS wave contains contributions from several products. The leading edge intensity is weighted by the associative desorption of

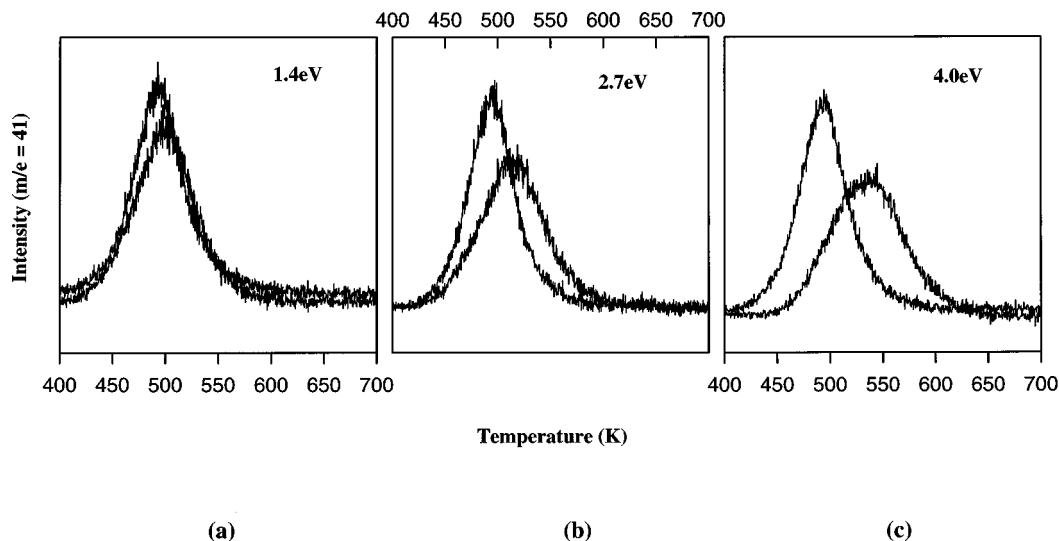


FIG. 3. TPR spectra of  $m/e=41$  taken before and after an exposure of  $\sim 1 \times 10^{16}$  collisions/cm<sup>2</sup> of a (a) 1.4 eV, (b) 2.7 eV, and (c) 4.0 eV xenon beam to an Al(111) surface at 300 K and saturated with isobutyl iodide.

diisobutyl iodide (DIBAI,  $T_{\max}$  at  $\sim 490$  K).<sup>41</sup> The latter portion of the peak is more heavily weighted by the desorption of isobutene (which is believed to be the predominant thermal reaction product) and diisobutyl aluminum hydride (DIBAH,  $T_{\max}$  at  $\sim 515$  K). The product partitioning is sensitive to coverage, but weakly varies at coverages within  $\sim 20\%$  of saturation. For this reason, a saturation coverage of isobutyl iodide was used in all the collision-induced reaction experiments reported here.

### The collision-induced reaction experiment

The collision-induced reaction experiments were performed at surface temperatures above 200 K to minimize effects due to the adsorption from the background gases during an experimental run. The exposures were made at 300 K and the sample subsequently cooled. The velocity distribution of each gas was recorded prior to the collision experiments. After reaching the desired exposure to the beam, TPR spectra were recorded at  $m/e=41$ . Control experiments were performed for each beam energy and exposure used by blocking the beam path with the shutter and exposing either the clean or adsorbate covered surface to the beam flux background. The TPR spectra obtained were identical to those taken for the same adsorbate coverage but without the beam exposure. This showed that no reaction or contamination results from indirect effusive gas load of the beam. Since the seeded beam mixture contained predominantly helium, we also examined the (remote) possibility of a reaction induced by helium atom collisions. In this control experiment, the adsorbate covered surface was exposed to a pure helium beam at various nozzle temperatures. No effect on the adsorbates was observed (the energy contained in the helium beam is  $<0.4$  eV).

### Observation and results of collision-induced reaction

Collision experiments were carried out in the energy range of 1–4 eV for the Xe beam. For Kr, the maximum

beam energy obtained was 2.7 eV while that for Ar was 1.4 eV. The thermally activated barrier for the  $\beta$ -hydride elimination reaction is estimated by TPRS to be in the range of  $\sim 1$  eV.<sup>37,41</sup> On varying the incident beam energy for Ar from 1 to 1.4 eV, only negligible changes were seen in the TPRS data for  $m/e=41$  (data not shown). This suggests an insignificant cross section for CID by the Ar atoms in this energy range. The net energy transfer is expected to depend on the incident mass and consequently so should the reaction cross section. Small, but measurable, reaction probabilities were observed for both 1.4 eV Kr and Xe beams. The representative TPR spectra shown in Fig. 3 were collected for Xe beams incident at three distinct energies. Figures 3(a)–3(c) show the effect of the normal energy component of the incident atom on the TPR data for a constant exposure of  $\sim 1 \times 10^{16}$  collisions/cm<sup>2</sup>. Isobutyl iodide physisorbs with an appreciable strength on the walls of the chamber and thus a low-level flux from the background is difficult to eliminate. The integrated beam fluxes used were restricted in part minimize errors due to adsorption from the background. Three major effects are evident in the data shown. First, there is a marked shift of the desorption peak towards higher temperatures with increasing beam energy. The measured shifts varied from  $\sim 10$  K for the 1.4 eV beam to  $\sim 50$  K for the 4 eV beam. Second, integration of the peak intensity suggests the yield of the desorbing products is reduced by  $\sim 2\%$ , 11%, and 18%, respectively, with increasing beam energy (at a constant integrated flux). Third, the collision process produces large changes in the TPRS line shapes. The magnitude of this change scales with the beam energy and, as we show below, the integrated flux as well.

The response of the TPRS data to varying exposures to the high energy Xe beam at 4 eV is demonstrated by the data shown in Fig. 4. The number of Xe collisions was varied over 1 order of magnitude in the range of  $1 \times 10^{15}$  to  $1 \times 10^{16}$  atoms/cm<sup>2</sup>. Both the maximum desorption temperature and the integrated desorption intensity vary progressively over the range of integrated fluxes used. These effects

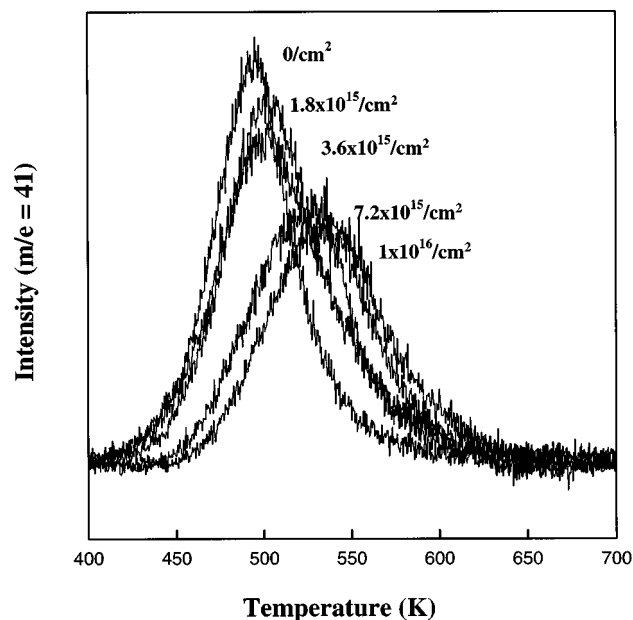


FIG. 4. TPR spectra of  $m/e = 41$  as a function of exposures of a 4 eV xenon beam to an Al(111) surface at 300 K and saturated (8 L) with isobutyl iodide. The values next to each spectrum indicate the total flux (collisions/cm<sup>2</sup>) exposures of the beam.

also are convolved with substantial changes in the line shapes of the TPR spectra. We defer further comments on these points until later.

As noted earlier, the thermal decomposition of isobutyl iodide on Al(111) produces, in addition to isobutene and dihydrogen, a variety of aluminum etching products, including AlI, DIBAI, and DIBAH, whose yields depend strongly on adsorbate coverage. We examined the influence of the

energetic Xe collisions on the relative desorption yield for each of these products in order to more fully understand the product partitioning seen in this reaction. Appropriate ionization fragments were chosen for monitoring the reactions yielding the most important products:  $m/e = 41$  (isobutene, isobutyl compounds);  $m/e = 2$  (dihydrogen);  $m/e = 141$  (DIBAH, DIBAI);  $m/e = 154$  (AlI);  $m/e = 168$  (DIBAI). The  $\beta$ -hydride elimination reaction occurs concurrently with the associative desorption of diisobutyl aluminum hydride and dihydrogen<sup>39</sup> and serves as the required source of surface-bound hydrogen. Selective activation of the  $\beta$ -hydride elimination reaction at 300 K by the collisional energy transfer is expected to influence the kinetics of (and hence TPRS data for) these reactions. Figures 5(a)–5(c) show TPR spectra for each of the noted masses taken before and after a 4 eV xenon beam exposure (corresponding to an integrated flux of  $\sim 1 \times 10^{16}$  collisions/cm<sup>2</sup>) at 300 K. From Fig. 5(a), it can be seen clearly that there is a large (almost 70%) reduction in the integrated peak intensity of  $m/e = 141$  desorption profile. The two peak profile of the initial state (due to a closely competitive desorption of diisobutyl aluminum iodide at  $\sim 490$  K and diisobutyl aluminum hydride at  $\sim 515$  K) is lost; it is replaced by a broad feature centered near  $\sim 515$  K. Figure 5(b) shows a similar and confirming decrease in the TPR spectra measured at  $m/e = 168$ , an ion specific to DIBAI. A reduction in the integrated intensity (again of about 70%) is seen for the main peak. A simultaneous emergence of another, albeit smaller, peak at  $\sim 425$  K is also evidenced. It is noteworthy that this feature is generated only at the upper end of the incident beam energies studied. The data suggest that xenon bombardment predominantly depletes states yielding DIBAI, although the promoted state at 425 K suggests the effects are kinetically very heterogeneous. Fig-

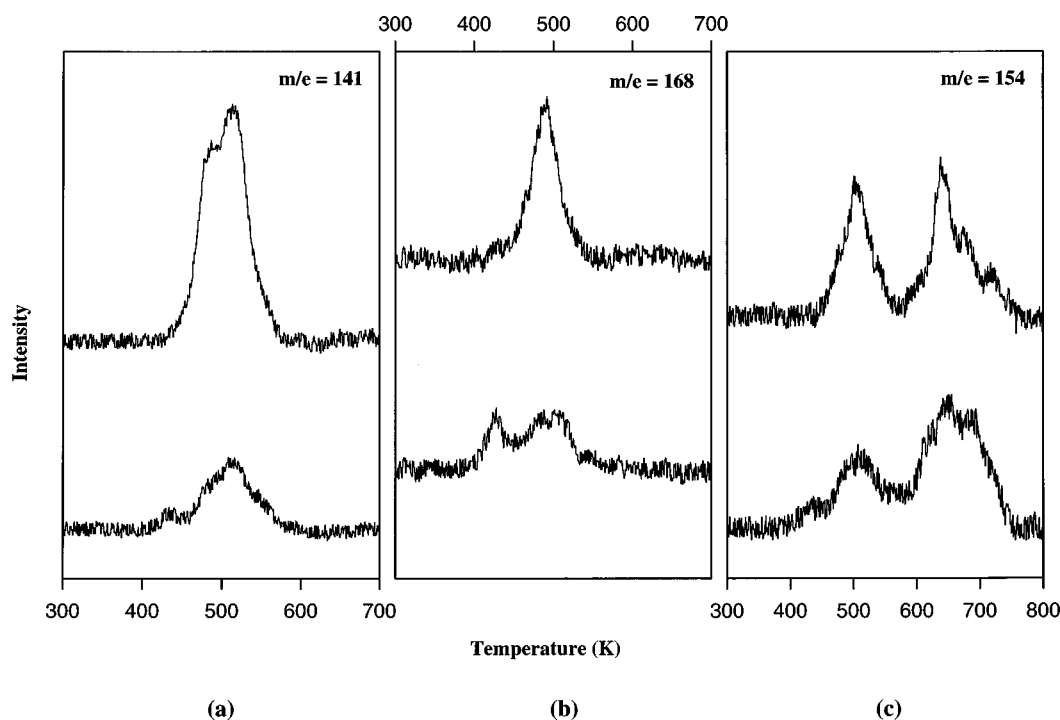


FIG. 5. TPR spectra of (a)  $m/e = 141$ , (b)  $m/e = 154$ , and (c)  $m/e = 168$  taken before (top spectra) and after (bottom spectra) an exposure of  $\sim 1 \times 10^{16}$  collisions/cm<sup>2</sup> flux of a 4 eV xenon beam to an Al(111) surface at 300 K and saturated with isobutyl iodide.

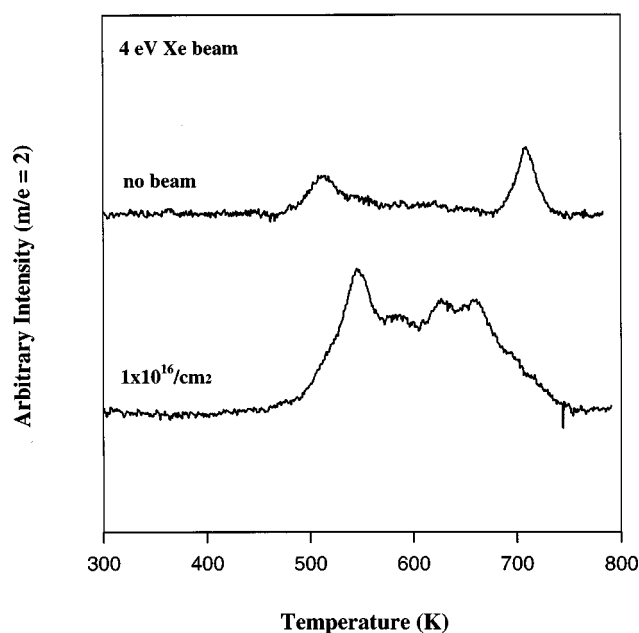


FIG. 6. TPR spectra of  $m/e=2$  taken before (top) and after (bottom) an exposure of  $\sim 1 \times 10^{16}$  collisions/cm<sup>2</sup> flux of 4 eV xenon beam to an Al(111) surface at 300 K and saturated with isobutyl iodide.

ure 5(c) shows data recorded for  $m/e=154$ , the  $\text{AlI}^+$  fragment. The data suggest, again, that low energy states yielding this fragment (ones due to DIBAI) are depleted. It is most interesting to note that the higher energy states (presumably representing the desorption of  $\text{AlI}$  as a stable diatomic molecule) are enhanced. The broad tailing seen on the high temperature feature is not understood but may be due to desorption of  $\text{AlI}$  from heterogeneous surface sites. The complex line shapes make integration difficult and, thus, no attempt has been made to quantify the changes in intensity seen here. The remaining product which results from the  $\beta$ -hydride elimination process is dihydrogen. Figure 6 shows desorption spectra of  $m/e=2$  taken before (upper curve) and after (lower curve) collision-induced activation with a  $1 \times 10^{16}$  atoms/cm<sup>2</sup> exposure of the 4 eV xenon atom beam. The “simple” pattern of the spectrum shown in the upper trace has been analyzed elsewhere.<sup>39</sup> The complexity of the desorption profile seen in the post collision spectrum (lower trace) is both intriguing and presently not understood. The possibility of the hydrogen coming from the adsorption of water from the background gases was ruled out by both mass spectroscopy (no increase in water peak intensity is observed in the residual gas analyzer during beam exposure) and AES (which shows no signs of any surface oxygen or Al–O bonding). One possibility we have considered but have not been able to firmly establish is that of multiple desorption states of hydridoaluminum halides ( $\text{AlH}_x\text{I}_{3-x}$ ). We defer further comment on this point to later.

The influence of the mass of the incident atoms in the collision dynamics was investigated using a substitution of Kr (Fig. 7) for Xe [Fig. 3(b)] in the seeded gas at fixed kinetic energy (2.7 eV) and gas dose ( $\sim 1 \times 10^{16}$  collisions/cm<sup>2</sup>). Comparison of these two figures shows that the more massive xenon has only a marginal dif-

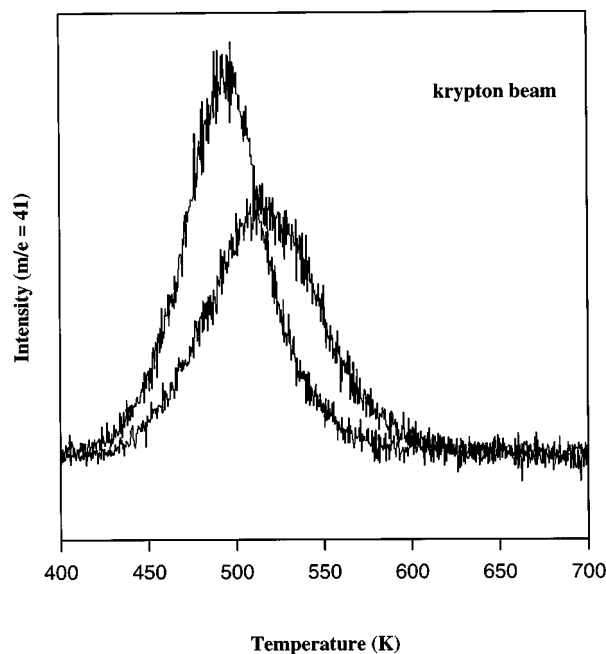


FIG. 7. TPR spectra of  $m/e=41$  for an Al(111) surface (at 300 K) saturated with isobutyl iodide and exposed to a constant flux of  $1 \times 10^{16}$  collisions/cm<sup>2</sup> for krypton at 2.7 eV.

ference viz. krypton at this energy. This conclusion was further supported by monitoring the behavior of the  $m/e=154$  desorption profile in an identical set of experiments (data not shown). The intensity and line shape changes seen in the 490 and 625 K peaks were similar.

An adsorbate covered surface maintained at a constant surface temperature during a collision experiment is under thermal equilibrium. Thermal energy participation is inconsequential for a process where the colliding species hits the surface from a distance in a rapid action. For example, in the collision-induced dissociation of methane on Ni(111),<sup>25</sup> the methane is propelled towards the surface with the energy acquired from the collision with the incident inert gas atom. In this billiard-ball-like mechanism, the surface energy plays no role (to a first approximation) in the dissociation process. We carried out collision-induced reaction experiments at two different surface temperatures (200 and 300 K) to test this hypothesis for isobutyl groups on Al(111). These data are shown in Fig. 8. For both experiments, a 4 eV Xe beam was used. At the lower surface temperature, the measured reduction in integrated intensity for a fixed integrated flux of Xe was always slightly less. Perhaps more interesting, the measured shift in peak maximum was  $\sim 50$  K at the higher surface temperature case but approaches  $\sim 80$  K in the 200 K experiment. Differences in peak broadening were also noted. It thus appears that a complex coupling of the incident and surface thermal energies is observed in this process.

## DISCUSSION

### The absolute cross section for collision-induced reaction of isobutyl iodide on Al(111)

Every reaction has a finite probability of occurrence for a given set of controlling parameters determined by the re-

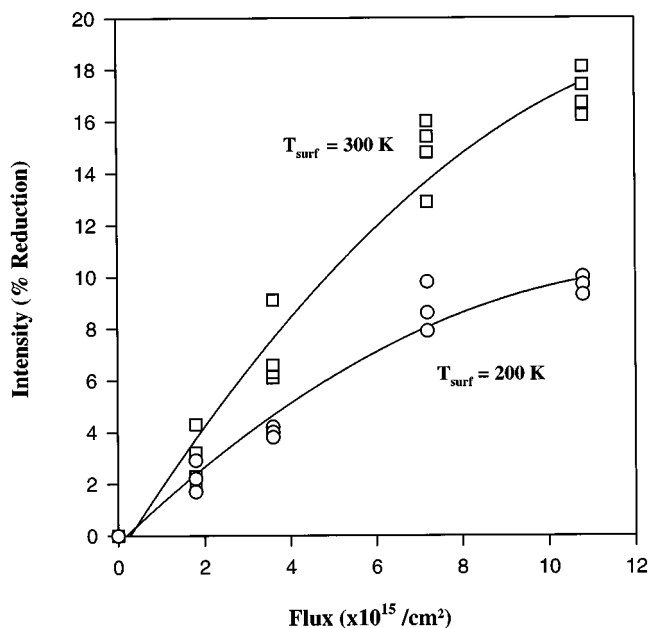


FIG. 8. Plot of reduction in integrated desorption intensity of  $m/e=41$  as a function total flux of 4 eV xenon beam incident on an Al(111) surface saturated with isobutyl iodide at 300 K (top curve) and 200 K (bottom curve), respectively.

action cross section.<sup>44</sup> The most-likely collision-induced reaction (CIR) in the present case (see below) is the unimolecular  $\beta$ -hydride elimination (i.e., dissociative conversion) of the isobutyl species to isobutene. The energy transfer and conversion therefore are given as



where  $E_i$  and  $E_f$  are the initial and the final energies of the colliding atom,  $B$ . We present a more detailed discussion of the dynamics and the constraints which preclude the thermal activation of more complex pathways via collisions in the hyperthermal energy range below. As noted above, Ar collisions of 1.4 eV were essentially incapable of activating any reaction for the integrated fluxes used. Both Kr and Xe collisions showed larger apparent cross sections, however. Figure 9 shows a more quantitative depiction of the energy scaling seen. The plot shows the experimentally measured reduction (in percent) in the integrated  $m/e=41$  TPRS intensity as a function of the integrated flux (i.e., the collision density) of the xenon beam at three different energy values ( $T_{\text{surf}}=300$  K). We discuss this energy scaling in detail below.

#### Collision-induced activation and the energy transfer dynamics

Using the data in Fig. 9 obtained at an integrated flux of  $\sim 7 \times 10^{15}$  collisions/cm<sup>2</sup> at each of the energies, the variation of the cross section was calculated as a function of the incident atom kinetic energy using the expression<sup>25,26</sup>

$$\Sigma_{\text{CIR}}(E_i) = \frac{\ln(\Theta_{\text{IB}}^{t=0}/\Theta_{\text{IB}}^{t=t})}{F_B t}, \quad (2)$$

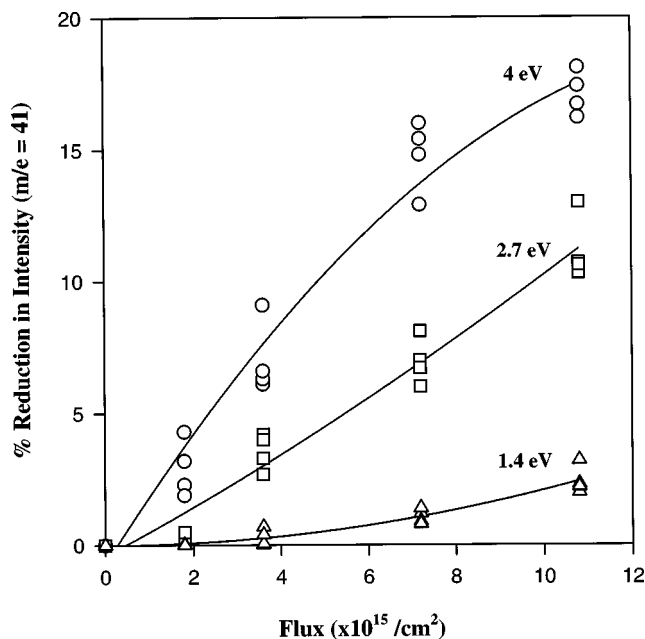


FIG. 9. Plot of percentage reduction in the integrated desorption intensity of  $m/e=41$  as a function of total flux exposure of 1.4, 2.7, and 4.0 eV xenon beam to an Al(111) surface at 300 K and saturated with isobutyl iodide.

where  $\Sigma_{\text{CIR}}$  is the absolute cross section for the collision induced reaction,  $\Theta_{\text{IB}}$  is the coverage of isobutyl groups at time  $t=0$  and  $t=t$ , and  $F_B$  is the absolute flux of the inert gas. The results are presented in Fig. 10.

Typically, the collision energy dependence of the reaction cross section,  $\Sigma_R(E)$ , can be approximated by an equation of the form<sup>45</sup>

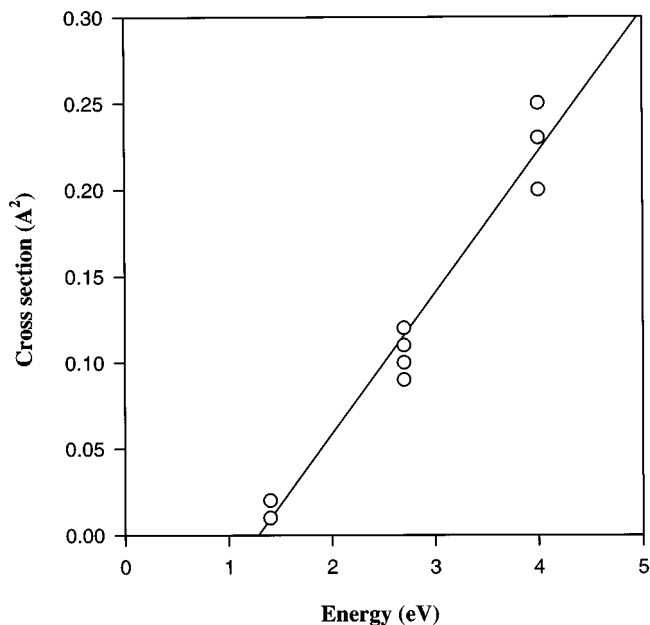


FIG. 10. Plot of  $\beta$ -hydride elimination reaction cross section ( $\text{\AA}^2$ ) as a function of the normal kinetic energy of the xenon beam incident on an Al(111) surface. The sample was dosed using a 8 L exposure of isobutyl iodide at 300 K. A constant flux of  $\sim 0.7 \times 10^{16}$  collisions/cm<sup>2</sup> was used to collect each data point.

$$\Sigma_R(E) = A \frac{(E - E_0)^n}{E}, \quad (3)$$

where  $E$  is the collision energy and  $A$  and  $n$  are fitting parameters. The translational energy threshold  $E_0$  for a chemical reaction can be defined as the minimum kinetic energy of the colliding species required for the reaction. In the present case,  $E_0$  corresponds to the minimum translational energy required of a colliding inert gas atom to overcome the activation barrier. Equation (3) is derived from a statistical treatment of simple gas-phase collision-induced dissociation events of the type  $A + BC \rightarrow A + B + C$ .<sup>46–50</sup> Fitting the data in Fig. 10 to this model, we estimate the threshold energy for the CID of the isobutyl groups, (presumably via a  $\beta$ -hydride elimination reaction) on the Al(111) surface to be  $\sim 1.1$  eV. The fitting parameter,  $n$ , has a value of 2 ( $\pm 0.2$ ). Values of  $n$  between 1–2.5 have been reported for a variety of gas phase, collision-induced dissociation systems based on both experimental<sup>27,51–53</sup> and theoretical studies.<sup>54</sup> The calculated threshold agrees well with that obtained from TPRS measurements of the decomposition of isobutyl iodide on single-crystalline aluminum surfaces,<sup>37</sup> where values of  $\sim 1$  eV on Al(111) and  $\sim 1.2$  eV on Al(100) were obtained. The close correspondence of the latter values to the threshold energy calculated here provides strong support for the inference that the CID of isobutyl moieties involves activation of only the unimolecular decomposition pathway (i.e.,  $\beta$ -hydride elimination).

The structures of the adsorbed isobutyl and iodine moieties (viz. coverage and, for the former, orientation) are not precisely known. Even so, it can be assumed that two types of collision events take place between the surface bound species and the colliding atoms. The collisions of the inert gas atoms occurring with either the isobutyl group or the iodine atom are bimolecular in nature. Collisions may also occur with the substrate atoms (a process whose formal molecular-ity depends on the kinetic energy of the incoming inert gas atom and the nature of the substrate). We consider first bimolecular collisions between the surface adsorbates and the inert gas atom. To a first approximation, the (direct) collision events can be modeled as being impulsive, where the energy transfer occurs in a hard sphere fashion without providing time for energy transfer to the internal modes. The corrugation depth of the attractive potential is not significant in comparison with the translational energy of the incoming atoms. The energy transfer from the inert gas atom to the adsorbate thus can be estimated as<sup>55</sup>

$$E_B^i = E_A^i (4m_B m_A / [m_B + m_A])^2, \quad (4)$$

where  $A$  and  $B$  correspond to the inert gas atom and the adsorbate species, respectively. We estimate the maximum energy transfer to be  $\sim 85\%$  for the isobutyl group and  $\sim 100\%$  for the iodine atom, respectively.

Having acquired this energy, the adsorbed moieties translate toward the aluminum substrate until they encounter the repulsive wall of the potential energy surface. It is therefore necessary to estimate how much energy the adsorbates lose to the surface. To determine this value, a secondary interaction is defined using a hard cube model.<sup>55</sup> The alumi-

num effective mass is used to account for the recoil effect. The energy that would be retained in the recoiling adsorbate species is given by

$$E_B^f = E_B^i (1 - 4m_B m_{\text{eff}} / [m_B + m_{\text{eff}}])^2, \quad (5)$$

where  $m_{\text{eff}}$  is the effective surface mass and is an approximation of the collective mass participating in the collision event.<sup>56,57</sup> This analysis predicts that the energy lost by the isobutyl group to the surface effective mass is  $\sim 100\%$  while that for the iodine atom is  $\sim 87\%$ . It therefore does not require an explicit calculation to show that the recoil energy is negligible in both the cases and is insufficient to overcome the adsorbate-surface bond strength.<sup>6</sup>

For both near-threshold desorption and sputtering, the collision events occur at either the topmost or second layer of the substrate and the minimum energy loss process corresponds to a mechanism in which the particle with the smallest mass moves within it.<sup>58</sup> The estimated threshold value for the incident energy which can bring about such a desorption of an isobutyl radical or iodine atom (where the bond energies are  $\sim 63$  kcal/mol<sup>35</sup> and  $\sim 80$  kcal/mol,<sup>59</sup> respectively) is much larger than the experimentally determined value and, thus, there appears little likelihood of effecting collision-induced desorption of either these species at these beam energies.

The third excitation process noted above involves the direct interaction of the colliding atom with the aluminum substrate atoms. A theoretical treatment of energy transfer between a hyperthermal inert gas atom and copper surface<sup>60</sup> yields a value of  $\sim 80\%$  in the range of energies appropriate to this study. Also, it was observed experimentally that the energy lost by a xenon atom with an incident energy of  $\geq 4$  eV, to a Pt or Au surface was  $\sim 60\%$ . Thus, for the scattering of Xe from Al, the energy transfer should be quite efficient. Assuming (based on these precedents) a broad range for the energy transfer to the surface of 60%–80% implies a value between 2.4–3.2 eV for the highest energy (4 eV) xenon beam. As a result, a ‘‘hot spot’’ could be formed and this, in turn, could result in an indirect energy transfer to the adsorbate. Zeiri *et al.*<sup>15,16</sup> noted for CIDE studies of  $N_2$  on a W surface that the importance of such a mechanism was insignificant. They proposed that the only indirect mechanism contributing to the desorption process was of a collision cascade type and only accounted for  $\sim 10\%$  of the total desorption yield.<sup>61</sup> We have shown above that, for a collision cascade mechanism to occur and cause either the desorption of aluminum atoms alone or of aluminum isobutyl species, the required threshold energy would be much larger than the values under consideration here. These arguments thus suggest that CID in this instance must predominantly involve a direct process.

The most intriguing fact noted in this work is the apparent coupling of the surface temperature to the translational energy transfer, as was suggested by the similar cross sections found for a 4 eV beam at a surface temperature of 200 K and a 2.7 eV beam at a surface temperature of 300 K. This implies that the lower  $k_B T$  factor is at least partially compensated by the translational energy of the colliding beam. A more quantitative analysis of the present data is complicated

both by the multiple reaction pathways which operate and the complex line shapes and peak shifts which accompany the beam exposure. The possibility of temperature and collision dependent modifications in structure of the adsorbed alkyl species has to be taken into consideration in a quantitative analysis since it would be a vital factor in determining the reaction kinetics and CID cross sections. These issues notwithstanding, it appears likely to us that the barrier to CID originates in the deformation and repulsive energies required to move the dissociating species close to the substrate (and is discussed below).<sup>21</sup>

Dubois *et al.*, have investigated the thermal stability and organization of alkyl groups on an aluminum surface by means of reflection-absorption infrared spectroscopy (RAIRS).<sup>62</sup> The surface bound isobutyl groups were derived both from the dissociation of isobutyl iodide as well as from the adsorption of triisobutyl aluminum (TIBA) on the surface. They report that the alkyl species maintained a temperature insensitive organization up to surface temperatures approaching the point of decomposition ( $\sim 450$  K). The TPRS data measured here (*viz.* line shape and  $T_{\max}$ ) show a significant sensitivity to the beam and thus suggest that changes in the orientation and organization of the chemisorbed isobutyl groups (and iodine atoms) likely result from the hyperthermal beam impact. These effects cannot be due to a simple annealing since thermal cycles below the decomposition threshold do not produce comparable changes in the TPR spectra.<sup>63</sup> The data therefore firmly establish that effects (presumably structural) other than those seen during thermal activation result from the CID process. These effects progressively complicate the thermal decomposition kinetics measured for the remaining adsorbed species by TPRS. We note, though, that the qualitative aspects of the product partitioning appear unchanged (at least for the conditions used here). It is interesting that, whatever the precise structural features which operate here, thermal annealing does not “undo” the lineshape and peak temperature effects seen in the post-exposure TPRS data. We believe this rate-structure sensitivity suggests an important role for nonequilibrium adsorbate overlayer structures in this system.

### Mechanism of collision-induced reaction and selectivity

We discussed the three pathways of energy transfer in the collision induced activation of isobutyl and iodine species in the previous section. The possibilities of a sputtering mechanism and radical desorption were ruled out on the basis of kinematic arguments. It is seen in the plot of cross section vs. incident beam energy (Fig. 9), that the threshold energy required for collision-induced activation is similar to the activation barrier for a  $\beta$ -hydride elimination reaction. However, the thermal chemistry of this system has other reactions with similar free energies of activation that also consume both aluminum and surface bound species at rates competitive with this particular process. Even so, iodine consuming reactions do not appear to be important. For example, the data presented in Fig. 3(c) shows that, although there is a change in line shape, there is little or no change seen in the integrated intensity of the broad set of peaks

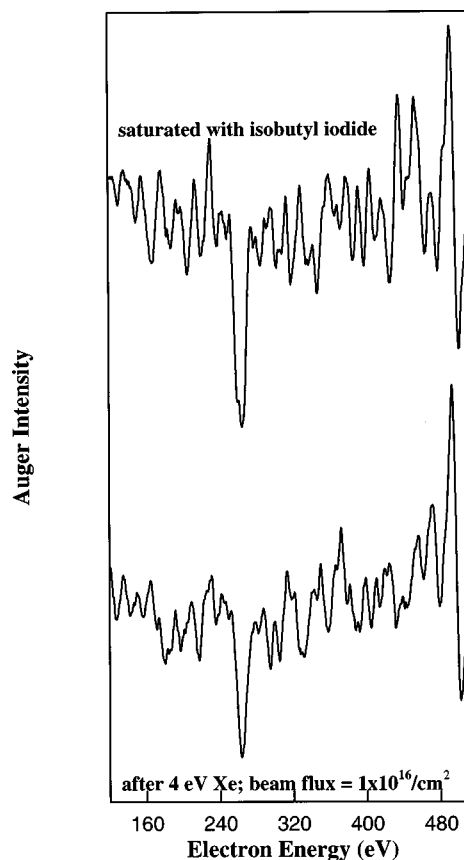


FIG. 11. Auger electron spectra of Al(111) surface; saturated with isobutyl iodide at 300 K and saturated with isobutyl iodide followed by exposure to a  $1 \times 10^{16}$  collisions/cm<sup>2</sup> flux of 4 eV xenon.

centered at  $\sim 625$  K (corresponding to  $AlI_x$ ) after the beam exposure. If the beam were inducing an iodine consuming reaction, the reduced iodine concentration on the surface would also have affected the formation of this product adversely. A further, albeit qualitative confirmation of this inference came from monitoring the surface by AES. Figure 11 shows AES data taken for an Al(111) surface under a variety of conditions (a low beam current was used to minimize electron-stimulated desorption). The upper panel is for a surface at 300 K saturated with isobutyl iodide. The second is a spectrum taken after exposing a similarly prepared surface to a 4 eV xenon beam with an integrated flux of  $\sim 1 \times 10^{16}$  collisions/cm<sup>2</sup>. The spectra, scaled to a common aluminum peak intensity to enable comparison of the relative intensities of C and I, show a clear reduction in the intensity of the C(KLL) peak at 272 eV and almost no change in intensity for the I(MNN) peak at 511 eV after the beam exposure. The decrease seen in the carbon coverage is approximately the same as that suggested by the TPRS results. The reduced concentration of the surface isobutyl groups as suggested by both AES and TPRS is expected to affect the associative product forming reactions in a quantitatively proportional manner. Post beam exposure desorption intensities (Fig. 5) do indeed show that the yields of aluminum containing ions are greatly reduced ( $m/e = 141$  and 168), with  $\sim 80\%$  reductions being seen for the maximum exposures used. Comparing this with the coverage dependent yields

seen in the TPRS experiments indicates that it matches well with the results obtained for an initial 2 L exposure of isobutyl iodide.<sup>64</sup>

The final issue we address is the mechanism of the collision-induced  $\beta$ -hydride elimination reaction. We noted earlier that the energy transfer is mass dependent and, for a large mass atom such as xenon, the impact should essentially crush the isobutyl groups. A similar mechanism was proposed by Ceyer *et al.*,<sup>25</sup> in which a dissociating methane molecule is trapped between the Kr (the highest mass used in that study) and a nickel surface. The deformation of the tetrahedral structure of the methane molecule caused by the impact brings the carbon closer to the metal surface and allows a hydrogen from the deformed C–H bond to tunnel to the metal surface. We believe a similar mechanism may be operating in the present system as well. Such mechanisms appear to be general, at least on the basis of the reports available in the literature which describe the CID of methane<sup>65–67</sup> and ethane<sup>65,68,69</sup> on various metal surfaces. It is interesting to note that, for the latter, the preferred dissociation is that of the C–H and not the C–C bond. Madix and McMaster<sup>68</sup> have shown that the experimental results are in excellent agreement with those predicted from the Eckart tunneling model<sup>70</sup> where the motion along the one-dimensional reaction coordinate for the lowest energy tunneling pathway are well represented by the Eckart potential. The activation of the  $\beta$ -hydride elimination reaction with a threshold energy as small as  $\sim 1.1$  eV, which coincides with the thermal activation barrier for the reaction, suggests that the reaction proceeds via a non-RRKM type mechanism.<sup>44</sup> If the reaction followed an equilibrium energy dissipation pathway, where the energy was distributed uniformly to all the internal modes, then the total energy required to activate the C–H bond would be much larger than is feasible via energy transfer from a hyperthermal neutral gas molecular beam. Since the interaction time of the colliding atom with the adsorbate is of the order of the vibrational lifetime, the collision can be viewed as being totally impulsive in nature. It is possible that the isobutyl fragment is oriented on the surface with its methyls pointing away from the surface (the RAIRS data are consistent with this picture).<sup>63</sup> A collision-based distortion would bring the activatable beta hydrogen and the surface into close proximity. Further development of this argument requires a more detailed knowledge of the structural aspects of the surface bound isobutyl groups than is currently available.

## ACKNOWLEDGMENT

We are grateful for the funding support for this project by the National Science Foundation (Grant Nos. CHE-9300995 and CHE-9626871).

<sup>1</sup>G. A. Somorjai, *Chemistry in Two Dimensions* (Cornell University Press, Ithaca, 1981).

<sup>2</sup>D. A. King, *CRC Crit. Rev. Solid State Mater. Sci.* **7**, 167 (1978).

<sup>3</sup>B. E. Bent, *Chem. Rev.* **96**, 1361 (1996).

<sup>4</sup>J. G. Ekerdt, Y. M. Sun, A. Szabo, G. J. Szulczewski, and J. M. White, *Chem. Rev.* **96**, 1499 (1996).

<sup>5</sup>J. R. Creighton and J. E. Parmeter, *Crit. Rev. Solid State Mater. Sci.* **18**, 175 (1993).

- <sup>6</sup>L. H. Dubois, B. E. Bent, and R. G. Nuzzo, *Surface Reactions*, edited by R. J. Madix, (Springer, Berlin, 1994), Vol. 34, p. 135.
- <sup>7</sup>M. K. Weldon and C. M. Friend, *Chem. Rev.* **96**, 1391 (1996).
- <sup>8</sup>S. T. Ceyer, D. J. Gladstone, M. McGonigal, and M. T. Schulberg, *Physical Methods of Chemistry*, 2nd ed., edited by B. W. Rossiter, and R. C. Baetzold (Wiley, New York 1993).
- <sup>9</sup>C. R. Arumainayagam and R. J. Madix, *Prog. Surf. Sci.* **38**, 1 (1992).
- <sup>10</sup>L. Q. Xia and J. R. Engstrom, *J. Chem. Phys.* **101**, 5329 (1994).
- <sup>11</sup>L. Q. Xia, M. E. Jones, J. N. Maity, and J. R. Engstrom, *J. Chem. Phys.* **103**, 1691 (1995).
- <sup>12</sup>K. A. Pacheco, B. A. Ferguson, C. Li, S. John, S. Banerjee, and C. B. Mullins, *Appl. Phys. Lett.* **67**, 2951 (1995).
- <sup>13</sup>S. R. Leone, *Jpn. J. Appl. Phys., Part 1* **34**, 2073 (1995).
- <sup>14</sup>Y. Zeiri, J. J. Low, and W. A. Goddard III, *J. Chem. Phys.* **84**, 2408 (1986).
- <sup>15</sup>Y. Zeiri, *Surf. Sci.* **231**, 404 (1990).
- <sup>16</sup>Y. Zeiri and R. R. Lucchese, *J. Chem. Phys.* **94**, 4055 (1991).
- <sup>17</sup>E. Vilallonga and H. Rabitz, *J. Chem. Phys.* **97**, 1562 (1992).
- <sup>18</sup>K. Yang, H. Cheng, E. Vilallonga, and H. Rabitz, *Surf. Sci.* **326**, 177 (1995).
- <sup>19</sup>J. D. Beckerle, A. D. Johnson, and S. T. Ceyer, *Phys. Rev. Lett.* **62**, 685 (1989).
- <sup>20</sup>J. D. Beckerle, A. D. Johnson, and S. T. Ceyer, *J. Chem. Phys.* **93**, 4047 (1990).
- <sup>21</sup>S. T. Ceyer, *Science* **249**, 133 (1990).
- <sup>22</sup>S. T. Ceyer, *Langmuir* **6**, 82 (1990).
- <sup>23</sup>J. D. Beckerle, A. D. Johnson, Q. Y. Yang, and S. T. Ceyer, *Solvay Conference on Surface Science* (Springer-Verlag, Berlin, 1988).
- <sup>24</sup>J. D. Beckerle, Q. Y. Yang, A. D. Johnson, and S. T. Ceyer, *J. Chem. Phys.* **86**, 7236 (1987).
- <sup>25</sup>J. D. Beckerle, A. D. Johnson, Q. Y. Yang, and S. T. Ceyer, *J. Chem. Phys.* **91**, 5756 (1989).
- <sup>26</sup>G. Szulczewski and R. J. Levis, *J. Chem. Phys.* **101**, 11070 (1994).
- <sup>27</sup>G. Szulczewski and R. J. Levis, *J. Chem. Phys.* **103**, 10238 (1995).
- <sup>28</sup>D. Velic and R. J. Levis, *J. Chem. Phys.* **104**, 9629 (1996).
- <sup>29</sup>L. Romm, T. Livneh, and M. Asscher, *J. Chem. Soc. Faraday Trans.* **91**, 3655 (1995).
- <sup>30</sup>J. R. Engstrom, D. A. Hansen, M. J. Furjanic, and L. Q. Xia, *J. Chem. Phys.* **99**, 4051 (1993).
- <sup>31</sup>M. E. Gross, L. R. Harriott, and R. L. Opila, Jr., *J. Appl. Phys.* **68**, 4820 (1990).
- <sup>32</sup>R. Jairath, A. Jain, M. J. Hampden-Smith, and T. T. Kodas, *CVD of Metal*, edited by M. J. Hampden-Smith and T. T. Kodas (VCH, Weinheim, 1995), p. 1.
- <sup>33</sup>B. E. Bent, R. G. Nuzzo, and L. H. Dubois, *Mater. Res. Soc. Symp. Proc.* **101**, 177 (1988).
- <sup>34</sup>B. E. Bent, R. G. Nuzzo, and L. H. Dubois, *Mater. Res. Soc. Symp. Proc.* **131**, 327 (1989).
- <sup>35</sup>B. E. Bent, R. G. Nuzzo, and L. H. Dubois, *J. Am. Chem. Soc.* **111**, 1634 (1989).
- <sup>36</sup>B. E. Bent, C. T. Kao, B. R. Zegarski, L. H. Dubois, and R. G. Nuzzo, *J. Am. Chem. Soc.* **113**, 9112 (1991).
- <sup>37</sup>B. E. Bent, R. G. Nuzzo, B. R. Zegarski, and L. H. Dubois, *J. Am. Chem. Soc.* **113**, 1137 (1991).
- <sup>38</sup>B. C. Wiegand, S. P. Lohokare, and R. G. Nuzzo, *J. Phys. Chem.* **97**, 11553 (1993).
- <sup>39</sup>G. Scoles, D. Bass, U. Buck, and D. Laine, *Atomic and Molecular Beam Methods* (Oxford University Press, New York, 1988), Vol. 1.
- <sup>40</sup>J. B. Anderson, *Molecular Beams and Low Density Gas Dynamics*, edited by P. P. Wegener (Marcel Dekker, New York, 1974).
- <sup>41</sup>S. P. Lohokare, E. L. Crane, L. H. Dubois, and R. G. Nuzzo, *Langmuir* **14**, 1328 (1998).
- <sup>42</sup>J. B. Anderson and J. B. Fenn, *Phys. Fluids* **8**, 780 (1965).
- <sup>43</sup>J. A. O'Hanlon, *User's Guide to Vacuum Technology* (Wiley, New York, 1980).
- <sup>44</sup>R. D. Levine and R. B. Bernstein, *Molecular Reaction Dynamics and Chemical Reactivity* (Oxford University Press, New York, 1987).
- <sup>45</sup>A. G. Urena, *J. Phys. Chem.* **96**, 8212 (1992).
- <sup>46</sup>R. D. Levine, *Chem. Phys. Lett.* **11**, 109 (1971).
- <sup>47</sup>R. D. Levine and R. B. Bernstein, *J. Chem. Phys.* **56**, 2281 (1972).
- <sup>48</sup>C. Rebeck and R. D. Levine, *J. Chem. Phys.* **58**, 3942 (1973).
- <sup>49</sup>E. E. Park, A. Wagner, and S. Wexler, *J. Chem. Phys.* **58**, 5502 (1973).
- <sup>50</sup>A. F. Wagner and E. K. Parks, *J. Chem. Phys.* **65**, 4343 (1976).
- <sup>51</sup>E. K. Parks, N. J. Hansen, and S. Wexler, *J. Chem. Phys.* **58**, 5489 (1973).

- <sup>52</sup>S. K. Loh, D. A. Hales, L. Lian, and P. B. Armentrout, *J. Chem. Phys.* **90**, 5466 (1989).
- <sup>53</sup>P. d. S. Claire, G. H. Peshherbe, and W. L. Hase, *J. Phys. Chem.* **99**, 8147 (1995).
- <sup>54</sup>W. J. Chesnavich and M. T. Bowers, *J. Phys. Chem.* **83**, 900 (1979).
- <sup>55</sup>E. K. Grimmelmann, J. C. Tully, and M. J. Cardillo, *J. Chem. Phys.* **72**, 1039 (1980).
- <sup>56</sup>Effective masses were determined experimentally through detailed scattering of inert gas atoms from platinum and gold surfaces. H. F. Winters, H. Coufal, C. T. Rettner, and D. S. Bethune, *Phys. Rev. B* **41**, 6240 (1990).
- <sup>57</sup>An approximate value of the effective mass can be obtained from the phonon dispersion and velocity of sound in the metal, however. The expression for the velocity of sound in metals is given by the Bohm-Staver relation:  $c^2 = (1/3)Z(m/M)v_F^2$ , where  $c$  is the velocity of sound,  $Z$  is the mass number,  $m$  is the mass of the electron,  $M$  is the mass of the atom and  $v_F$  is the Fermi velocity. Since the electron-ion mass ratio is typically of the order  $10^{-4}$  or  $10^{-5}$ , this predicts a sound velocity about 1% of the Fermi velocity, or of order  $10^4$  m/s. Therefore, in the typical interaction time period of  $\sim 30$ – $50$  fs, the phonons interact with a region  $3$ – $5$  Å wide. The lattice constant for aluminum is  $4.02$  Å. Hence, at the high energies under consideration, the effective mass of the metal is only of the order of  $1$ – $2$  atomic masses. By way of reference, an effective mass of one Al atom was estimated from the collision-induced dissociation dynamics of Al clusters. N. W. Ashcroft and N. D. Mermin, *Solid State Physics* (Cornell University Press, Ithaca, 1976).
- <sup>58</sup>Y. Yamamura, T. Takiguchi, and H. Kimura, *Nucl. Instrum. Methods Phys. Res. A* **78**, 337 (1993).
- <sup>59</sup>M. W. M. Hisham and S. W. Benson, *J. Am. Chem. Soc.* **91**, 3631 (1987).
- <sup>60</sup>The role of the surface temperature in the energy exchange can be estimated on the basis of a hard-cube model analysis along the lines of one performed for argon scattering from a tungsten surface by Grimmelmann *et al.* (Ref. 55). The final energy of the scattering atom is given by  $\langle E_g' \rangle = \alpha_g \langle E_g \rangle + \alpha_s \langle E_s \rangle$ , where  $\langle E_g' \rangle$  is the final average energy of the scattered atom,  $E_g$  is the incident energy,  $E_s$  is the surface energy ( $= 2k_B T$ ). The parameters  $\alpha_g$  and  $\alpha_s$  are derived on the basis of energy and momentum conservation  $\alpha_g = (1 - [4\mu/(\mu + 1)^2] \cos^2 \theta)$ ,  $\alpha_s = \mu(2 - \mu)/(\mu + 1)^2$ , where  $m = m/M$ , with  $m$  being the effective mass of the surface atoms influenced by the collision and  $M$  is the mass of the colliding atom. The value of  $k_B T$  for  $T = 273$  K is only  $2.35 \times 10^{-2}$  eV (Ref. 57). It can be easily seen as a result that the contribution from the surface temperature to the final energy of the scattering atom is not significant as compared to the incident translational energy of that atom. Hence, for all practical purposes the surface temperature factor can be neglected safely as we have already done in Eq. (3). H. Gades and H. M. Urbassek, *Appl. Phys. A* **61**, 39 (1995).
- <sup>61</sup>Y. Zeiri, A. Redondo, and W. A. Goddard III, *Surf. Sci.* **131**, 221 (1983).
- <sup>62</sup>B. R. Zegarski and L. H. Dubois, *Surf. Sci. Lett.* **262**, 129 (1992).
- <sup>63</sup>Iodine might act to block sites in what would be considered a “cage effect” on the remaining species. The consequence this would have on surface diffusion and reaction has not been established. C. J. Jenks, A. Paul, L. A. Smoliar, and B. E. Bent, *J. Phys. Chem.* **98**, 572 (1994).
- <sup>64</sup>This is reflected in the reduction obtained for  $m/e = 41$  TPRS intensities as well. It is observed that the intensity reduction for this mass is  $\sim 18\%$  in the case of CID which is in close agreement with the difference between the integrated TPRS intensities corresponding to 8 and 2 L exposures ( $\sim 20\%$ ) obtained from the exposure dependent thermal experiments.
- <sup>65</sup>R. W. Verhoef, D. Kelly, C. B. Mullins, and W. H. Weinberg, *Surf. Sci.* **311**, 196 (1994).
- <sup>66</sup>G. R. Schoofs, C. R. Arumainayagam, M. C. McMaster, and R. J. Madix, *Surf. Sci.* **215**, 1 (1989).
- <sup>67</sup>M. B. Lee, Q. Y. Yang, and S. T. Ceyer, *J. Chem. Phys.* **87**, 2724 (1987).
- <sup>68</sup>M. C. McMaster and R. J. Madix, *Surf. Sci.* **294**, 420 (1993).
- <sup>69</sup>D. J. Oakes, H. E. Newell, F. J. M. Rutten, M. R. S. McCoustra, and M. A. Chesters, *J. Vac. Sci. Technol. A* **14**, 1439 (1996).
- <sup>70</sup>R. P. Bell, *The Tunnel Effect in Chemistry* (Chapman and Hall, London, 1978).